Special Report

For reprint orders, please contact: reprints@futuremedicine.com

Nanomedicine

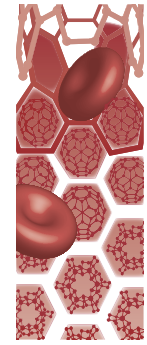

The importance of spheroids in analyzing nanomedicines' efficacy

Inês Mó[‡,1], Ivo J Sabino[‡,§,1], Duarte de Melo-Diogo[**,‡,1], Rita Lima-Sousa[1], Cátia G Alves[1] & Ilídio J Correia[*,1,2]

[1]CICS-UBI – Centro de Investigação em Ciências da Saúde, Universidade da Beira Interior, 6200-506, Covilhã, Portugal

[2]CIEPQPF – Departamento de Engenharia Química, Universidade de Coimbra, 3030-790, Coimbra, Portugal

*Authors for correspondence: icorreia@ubi.pt

**Authors for correspondence: demelodiogo@fcsaude.ubi.pt

[‡]Authors contributed equally

[§]Dedicated to the loving memory of Quirino Sabino

The use of nanomedicines for cancer treatment holds a great potential due to their improved efficacy and safety. During nanomedicines' preclinical *in vitro* evaluation stage, these are mainly tested on cell culture monolayers. However, these 2D models are an unrealistic representation of the *in vivo* tumors, leading to an inaccurate screening of the candidate formulations. To address this problem, spheroids are emerging as an additional tool to validate the efficacy of new therapeutics due to the ability of these 3D *in vitro* cancer models to mimic the key-features displayed by *in vivo* solid tumors. In this review, the application of spheroids for the evaluation of nanomedicines' physicochemical properties and therapeutic efficacy is discussed.

First draft submitted: 7 February 2020; Accepted for publication: 25 March 2020; Published online: 18 June 2020

Keywords: 2D *in vitro* models • 3D models • cancer/oncology • nanomaterials • spheroids • therapeutics

Conventional cancer treatments (e.g., radiotherapy and chemotherapy) are generally associated with off-target toxicity and low efficacy, leading to a poor therapeutic outcome [1,2]. To mitigate these limitations, researchers have been developing nanomedicines for application in cancer therapy [1,3,4]. Due to their physicochemical properties (size, surface charge, shape and corona composition), these nanomaterials can achieve a high tumor uptake and become internalized by cancer cells (reviewed in detail in [5–8]). In this way, nanomaterials can potentially mediate an anticancer effect with a higher efficacy and specificity toward cancer cells [9–13].

During nanomedicines' development, their efficacy is initially screened in 2D *in vitro* cancer models (monolayers of cells). Usually, these models are used to study nanomedicines' internalization in cancer cells and to determine their therapeutic efficacy [10,14–20]. Furthermore, the 2D cultures have also been used to select the candidate formulations to be assayed in the *in vivo* studies [21–23]. However, these 2D models are unable to mimic the 3D organization/architecture of the *in vivo* tumors nor its main drug resistance mechanisms [24–27]. In this way, the sole use of cell monolayers in the preclinical *in vitro* testing stage leads to the selection of candidates that may display a low therapeutic efficacy *in vivo* [28,29].

To address this bottleneck of the drug discovery process, 3D *in vitro* cancer models emerged as an additional platform to validate the efficacy of new therapeutics [30–34]. These models include the scaffold-based 3D cultures which are assembled by culturing cells in hydrogel-like structures, in inserts or in sponges (acellular 3D artificial matrices) [27,35]. On the other hand, the nonscaffold-based 3D cultures are attained through the formation of cellular aggregates using different methodologies such as the liquid overlay or hanging drop techniques [27,36,37]. Among the different 3D *in vitro* cancer models, spheroids (3D tightly-bond cellular aggregates) have been receiving an increasing attention from researchers [25,27,38]. Spheroids can mimic several features of the *in vivo* solid tumors, namely their: layered organization (composed by proliferative, quiescent and necrotic zones); gradients of nutrients, pH (due to spheroids' acidic core, the pH in spheroids can range from 7.2 in the periphery to 6.5 in the interior) and gases (the oxygen content, depending on the measured zone, can range from 50 up to 130 mmHg [39]);

Future Medicine

extracellular matrix (ECM) deposition; and cellular heterogenicity (spheroids can be assembled using cancer and stromal cells) [27,40,41]. Such features confer spheroids resistance to nanotherapeutics' activity and penetration [10,42–47]. In this way, spheroids are now being used as a tool to bridge the gap between 2D *in vitro* and *in vivo* cancer models [38,48,49].

In this review, the application of spheroids for assessing the efficacy of nanomedicines is analyzed. Initially, the properties of the spheroids are briefly overviewed. Then, the applicability of spheroids in the optimization of nanomedicines' physicochemical properties, as well as in the evaluation of nanomedicines' therapeutic efficacy are reviewed. At last, an outlook about the state of the art and the future directions are presented.

Properties of spheroids

Large spheroids (>500 μm) are cellular aggregates that can mimic the solid tumors' 3D structure, cell–cell and cell–ECM interactions, as well as the gradients of oxygen, pH and nutrients – Figure 1. Due to these features, spheroids display a resistance to therapeutics quite similar to that occurring in solid tumors – extensively reviewed elsewhere [27,36,49,50]. The techniques used to produce spheroids are also reviewed in detail in [25,27,36,40].

Spheroids display a three-layered organization, containing proliferative, quiescent and necrotic cells [51,52]. Spheroids' outer layer is composed of highly proliferative cells with unrestricted access to oxygen and nutrients [51]. On the other hand, quiescent cells are found in the spheroids' middle layer, while necrotic cells are present in spheroids' inner layer (core), being deprived of oxygen and nutrients [51–53]. In this way, cells in spheroids' interior are weakly affected by pharmaceuticals that act by suppressing cells' proliferation (e.g., paclitaxel) [24,54]. In turn, spheroids' hypoxic environment leads to: an upregulation of the expression of HIF-1α (which has been linked to an upregulation of antiapoptotic proteins and P-glycoprotein – a major drug efflux transporter that contributes to drug resistance); resistance to therapeutics whose action relies on the production of reactive oxygen species (e.g., doxorubicin [DOX]); acidification of the spheroids' core (as a result of the conversion of pyruvate to lactate to obtain energy – Warburg effect) [55–57].

The acidic environment found within spheroids affects the penetration and uptake of therapeutics [57–59]. This penetration barrier is also supported by the ECM components (e.g., collagen and elastin) secreted by the spheroids' cells as well as by the cell–cell and cell–ECM physical interactions occurring in spheroids [60,61]. These interactions are responsible for the establishment of a high interstitial fluid pressure that hinders therapeutics' penetration [60,62]. As importantly, the cell–cell interactions established between the cancer cells, cancer stem cells and stromal cells occurring within spheroids can enable signaling pathways enrolled in therapeutics' resistance, namely the HIF-1 and NOTCH pathways [36,63–65]. The PI3K-AKT-mTOR, ERK and MEK pathways are also established in spheroids [24,66].

Owing to these reasons, spheroids are now starting to be used for the screening of nanomedicines (reviewed in the subsequent sections).

Application of spheroids in the optimization of nanomedicines' physicochemical properties

During nanomedicines' development, their physicochemical properties, namely size, surface charge, shape and corona composition, must be optimized. These attributes play a crucial role in nanomedicines' biodistribution (reviewed in detail in [5–8]). After intravenous administration, nanomedicines must avoid rapid blood clearance (mediated by the kidneys, liver and spleen) and then must extravasate to the tumor tissue, penetrate the tumor mass and be internalized by cancer cells. The uptake of nanomedicines by cancer cells generally occurs by pinocytosis [67]. Depending on the nanomedicines' physicochemical properties, they can become internalized in cancer cells through clathrin-dependent endocytosis and/or clathrin-independent endocytosis, being the latter subdivided in: caveolae mediated endocytosis; clathrin- and caveolae-independent endocytosis; and micropinocytosis (reviewed in detail in [67,68]). Due to spheroids' structural similarities with the *in vivo* solid tumors, they can be used to predict nanomedicines' tumoral penetration capacity and therefore their optimal physicochemical properties (Figure 2) [33].

Nanomedicines' size

Spheroids have been extensively used for the optimization of nanomedicines' size [42,60,69–75]. In this regard, Huang *et al.* investigated the penetration of tiopronin-coated gold nanoparticles of size averaging 2, 6 and 15 nm into MCF-7 spheroids [42]. Due to their smaller size, the 2 and 6 nm sized-gold nanoparticles were able to diffuse throughout the spheroids (Figure 3). In contrast, the 15 nm-sized gold nanoparticles remained in the spheroids' outer layer, suggesting that their bigger size hinders their penetration into the spheroids' core. Interestingly, the

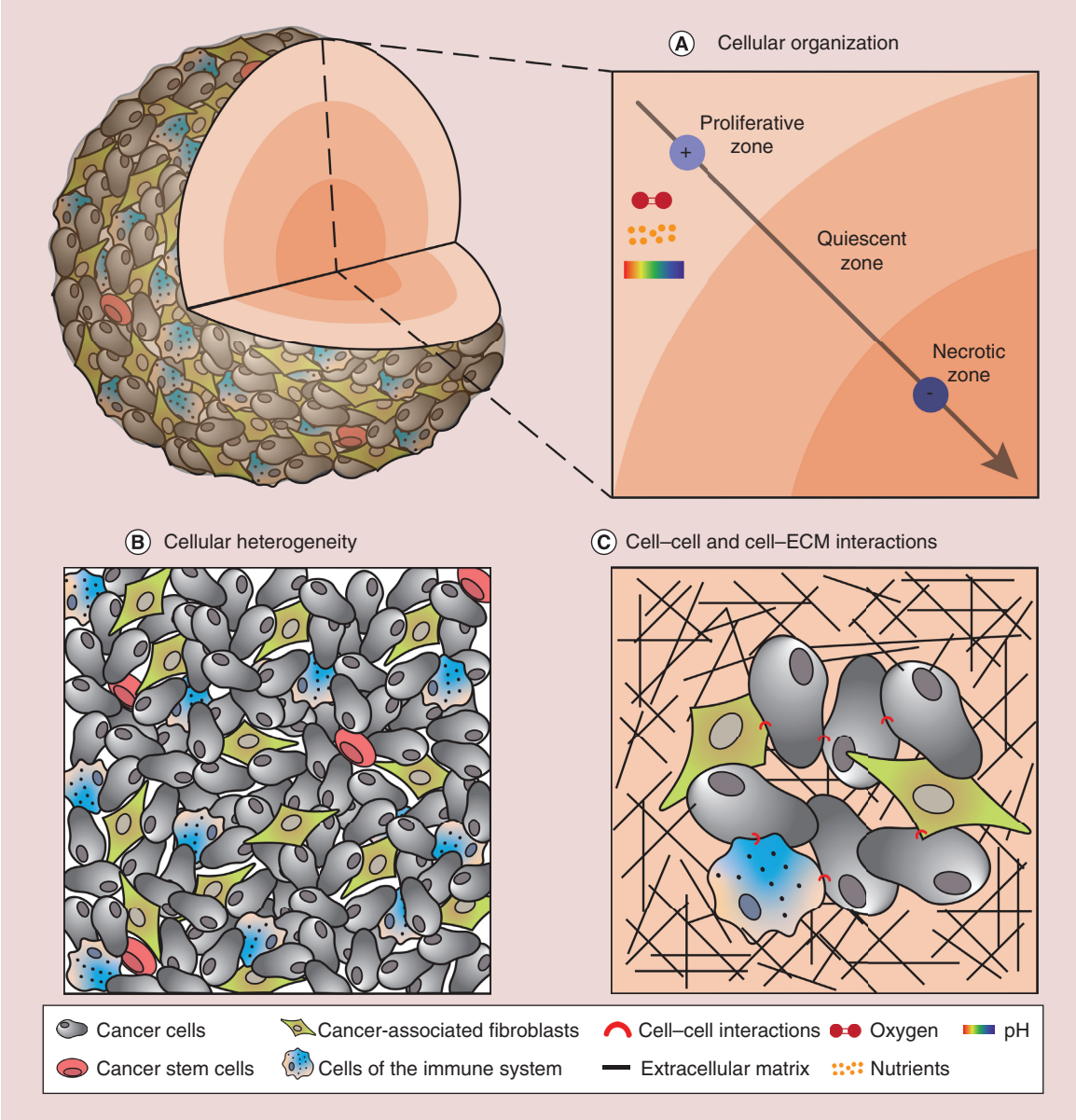

Figure 1. Schematic representation of spheroids' properties. (A) Spheroids display a three-layered organization with gradients of oxygen, nutrients and pH. **(B)** Representation of the cellular heterogeneity and **(C)** cell–cell and cell–ECM interactions occurring in the spheroids.
ECM: Extracellular matrix.

2 nm-sized gold nanoparticles also achieved the highest accumulation in the spheroids. These results were further confirmed *in vivo*, being observed that the smaller nanoparticles have a higher tumor uptake.

Goodman *et al.* used SiHa spheroids for investigating the optimal size of carboxylated polystyrene nanoparticles [60]. Their results revealed that the 20 nm sized nanoparticles achieve the highest accumulation in the spheroids' core, being followed by their equivalents with a size of 40 nm. In turn, the nanoparticles with 100 and 200 nm of size only became accumulated at spheroids' periphery, and thus were not able to penetrate to the spheroids' core. A similar trend was observed for thioether-bridged mesoporous organosilica nanoparticles [70]. In this study, the 20 nm-sized particles achieved the highest penetration into the U87MG spheroids, followed by their equivalents with 40 nm. In contrast, the 60 and 100 nm-sized mesoporous organosilica nanoparticles were found to accumulate mostly on the spheroids' outer layer. This trend was also confirmed *in vivo*, in which the 20 nm-sized nanoparticles achieved a deep and uniform distribution throughout the tumor tissue.

10.2217/nnm-2020-0054

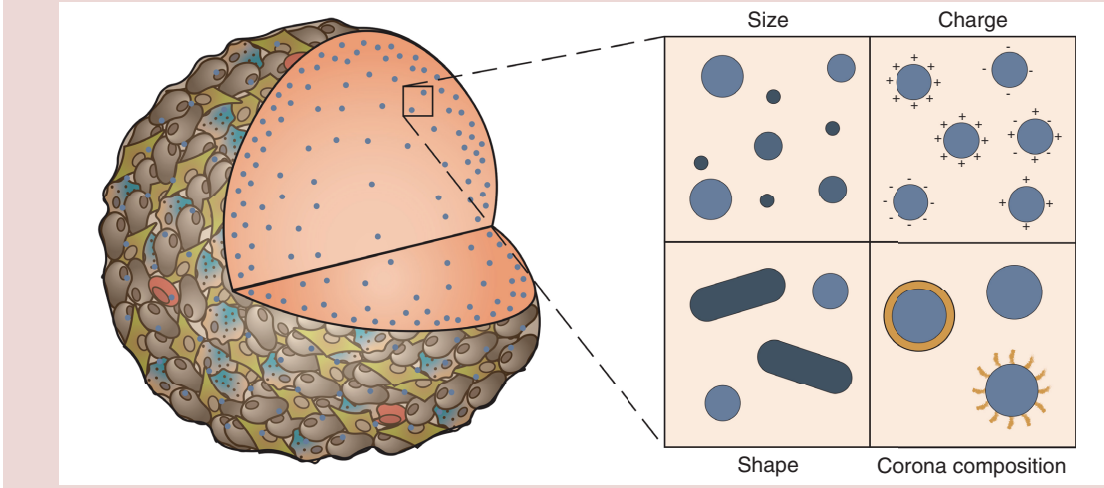

Figure 2. Schematic representation of the different nanomedicines' physicochemical properties influencing their penetration into spheroids.

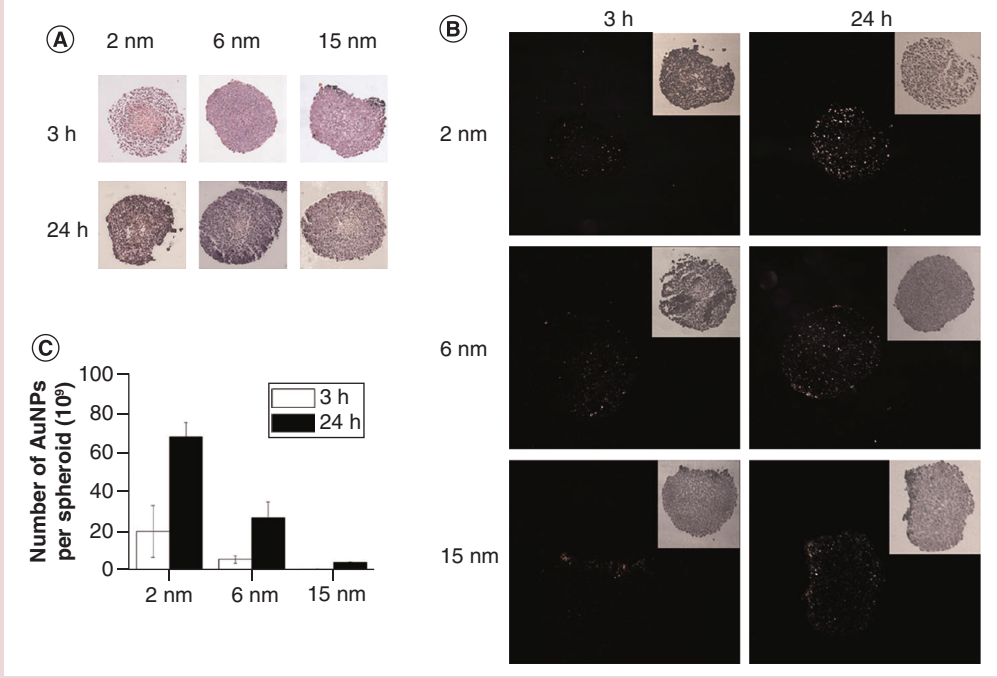

Figure 3. Influence of tiopronin-coated gold nanoparticles' size in their penetration into spheroids. (A) Images of hematoxylin and eosin stained spheroids and **(B)** dark field images of spheroids after incubation with the AuNPs. **(C)** Number of AuNPs per spheroid.
AuNP: Tiopronin-coated gold nanoparticle.
Reproduced with permission from [42], © American Chemical Society (2012).

Nanomedicines' charge

The impact of the nanomaterials' surface charge on their ability to penetrate spheroids has also been a studied subject [43,76–81]. In this regard, Jiang group demonstrated that negatively charged polystyrene-based nanoparticles (ζ potential of -34.9 mV) have a better ability to penetrate HepG2 spheroids when compared with their positively

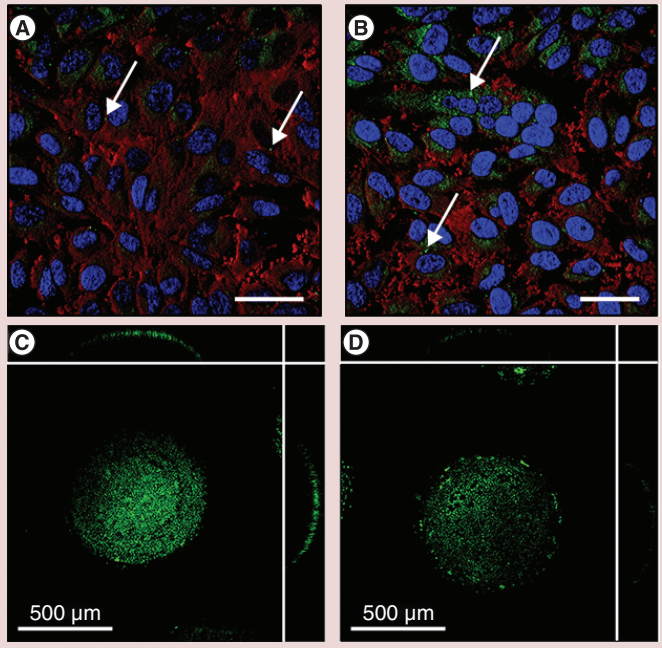

Figure 4. Influence of the mesoporous silica-based nanostructures' shape in their uptake by cancer cells and penetration into spheroids. Internalization of **(A)** sphere and **(B)** rod-shaped mesoporous silica-based nanostructures in monolayers of HeLa cells. The white arrows indicate the internalized nanostructures. Scale bar corresponds to 50 µm. Penetration of **(C)** sphere and **(D)** rod-shaped mesoporous silica-based nanostructures into spheroids. Blue channel: Hoechst 33342® stained cell nucleus; red channel: WGA-Alexa Fluor® 594 conjugate for cell cytoplasm staining; green channel: Dox fluorescence.
Reproduced with permission from [83], © The Royal Society of Chemistry (2016).

charged equivalents (+9.2 mV) [43]. In another work, Wang *et al.* analyzed the accumulation of lipid/poly(ethylene glycol) (PEG)-poly(lactic acid) (PLA) hybrid nanoparticles with different surface charges in the interior of MDA-MB-231 spheroids [76]. In this case, the cationic hybrids (+21.5 to +23.5 mV) were located at the periphery and interior of the spheroids. In contrast, the neutral (-9 and -8 mV) and anionic hybrids (-22.2 mV) had a weak penetration into the spheroids' core.

Nanomedicines' shape

Spheroids are also a valuable tool in the process of fine-tuning the shape of nanomaterials [82–86]. Zhao *et al.* verified that sphere-shaped fructose-coated nanoparticles achieve a higher uptake by MCF-7 spheroids [82], followed by those with a rod-shape and then by the vesicle-shaped ones. Dias *et al.* reported that rod-shaped mesoporous silica-based structures mediate a higher DOX delivery to HeLa cells when compared with their spherical equivalents [83] (Figure 4A & B). In contrast, when tested in HeLa spheroids, the sphere-shaped nanostructures were able to deliver a higher DOX payload with a uniform distribution throughout the spheroids (Figure 4C & D).

Nanomedicines' corona composition

Spheroids can also be used for the examination of the optimal surface coating of nanomedicines [44,73,87–97]. Steinbach-Rankins group analyzed the penetration of poly(lactic-*co*-glycolic acid) (PLGA) nanoparticles modified with PEG (a stealth agent), VIM (a tumor targeting cell penetrating peptide), MPG (a cell penetrating peptide) and MPG/PEG in HeLa spheroids [44]. In general, the coating of the PLGA nanoparticles enhanced their accumulation in spheroids. However, the PLGA nanoparticles coated with VIM, MPG and MPG/PEG were mostly accumulated at spheroids' outer layer. In stark contrast, PEG-coated PLGA nanoparticles were the best performing formulation since these were able to penetrate deep into HeLa spheroids. Sarisozen *et al.* demonstrated that the capacity of PEGylated micelles to penetrate NCI-ADR-RES spheroids is increased by functionalizing the micelles' surface with transferrin [98].

10.2217/nnm-2020-0054

In another work, Jiang group demonstrated that the delivery of DOX mediated by chitosan nanoparticles and by phenylboronic acid-functionalized chitosan nanoparticles to 2D cultures of SH-SY5Y cells was very similar [87]. On the other hand, the screening performed in SH-SY5Y spheroids suggested that the phenylboronic acid-functionalized chitosan nanoparticles may have better DOX deliver capabilities to all the three layers of the spheroids. Folate and PEG dual-functionalized chitosan-based nanoparticles were able to induce GFP expression in deeper cells of HeLa spheroids when compared with their equivalents only functionalized with PEG (Figure 5) [88].

Application of spheroids in the screening of nanomedicines' therapeutic efficacy

The end point of spheroids' application in the screening of nanomedicines' potential is to determine their therapeutic efficacy. In general, spheroids have been used to evaluate nanomedicines' mediated chemotherapy [46,99–102], radiotherapy [103–105], photothermal therapy [106–108], photodynamic therapy [109–112] and gene delivery [88,113,114].

Due to spheroids' similarities with the *in vivo* solid tumors, the therapeutic efficacy of nanomedicines toward this 3D *in vitro* cancer model is commonly inferior to that attained in 2D cell cultures. In this context, Oliveira *et al.* screened the therapeutic capacity of D-α-tocopheryl polyethylene glycol 1000 succinate (TPGS)-coated solid lipid nanoparticles loaded with DOX and α-Tocopherol succinate in spheroids [115]. When tested on 2D cultures of resistant human ovarian carcinoma cells (NCI/ADR), the dual drug-loaded solid lipid nanoparticles could reduce their viability to about 15% at a DOX dose of 8 μM. In stark contrast, this nanoformulation required a DOX dose of 100 μM to reduce NCI/ADR spheroids' viability to 34%. In another work, the IC_{50} of glyceryl monooleate coated Fe_3O_4 nanoparticles incorporating curcumin and temozolomide toward T-98G spheroids was approximately 75-times higher than that obtained in T-98G monolayers (5.22 vs 0.07 μg/ml) [45]. Interestingly, the synergism of the dual-drug loaded Fe_3O_4 nanoparticles was also inferior on spheroids (combination index of 0.47) when compared with that obtained in the 2D cultures (combination index of 0.24). Sarisozen *et al.* also reported that DOX-loaded micelles are able to reduce U87MG cells' viability to approximately 21% but that only decrease U87MG spheroids' viability to approximately 77% [46].

Spheroids may also be useful to determine the type of therapeutic approach with the most promising outcome. For instance, U87 cells suffered a similar reduction on their viability (to ~7–16%) upon treatment with PEGylated reduced graphene oxide mediated chemotherapy, photodynamic therapy and photothermal therapy [47]. In stark contrast, PEGylated reduced graphene oxide mediated chemotherapy and photodynamic therapy only reduced U87 spheroids' viability to approximately 40 and 56%, respectively. On the other hand, the photothermal therapy mediated by PEGylated reduced graphene oxide decreased spheroids' viability to approximately 18%, highlighting the enhanced potential of this therapeutic modality. In a recent work by Alves *et al.*, the photothermal effect mediated by IR780 loaded hyaluronic acid-based nanoparticles, at an IR780 dose of 3.5 μg/ml, could reduce MCF-7 cells' viability to 59% (Figure 6A) [10]. However, this therapeutic modality was unable to affect MCF-7 spheroids (viability ~100%) even at a 5 μg/ml dose of IR780. In stark contrast, the chemophotothermal therapy mediated by DOX- and IR780-loaded hyaluronic acid-based nanoparticles (IR780 dose: 5 μg/ml; DOX dose: 2.76 μg/ml) were effective on MCF-7 spheroids, by decreasing their viability to 34% (Figure 6B).

Conclusion & future perspective

In this review, the application of spheroids for the optimization of the nanomedicines' physicochemical properties was highlighted. In this regard, nanomedicines' size, surface charge, shape and corona composition could be fine-tuned by analyzing nanostructures' penetration into spheroids. In many cases, the leading nanoformulation behaved differently in spheroids and in cell monolayers. As importantly, the trends observed using the spheroids revealed a good correlation with the nanomedicines' *in vivo* behavior. Additionally, the use of spheroids for determining the therapeutic capacity of nanomedicines was also discussed. In general, nanomedicines were less effective toward spheroids comparatively to the effects observed in cell culture monolayers. In fact, in some cases, nanomedicines did not induce any therapeutic effect when tested on spheroids, clearly highlighting the importance of using spheroids in nanomedicines' drug discovery.

Despite of the advantages of using spheroids in the screening of nanomedicines, these are not yet routinely used in most laboratories. Such can be explained by the fact that spheroids' assembly is not as straightforward as seeding cell monolayers. Furthermore, the characterization equipment (e.g., fluorescence microscopes) and techniques (e.g., viability assays) available in most labs are not well-fitted or standardized for the analysis of spheroids. Due to these constraints, most of the developed spheroids also display a size that is lower than that of solid tumors in order to ensure spheroids' compatibility with the currently available high-throughput screening methods [37,116]. In the

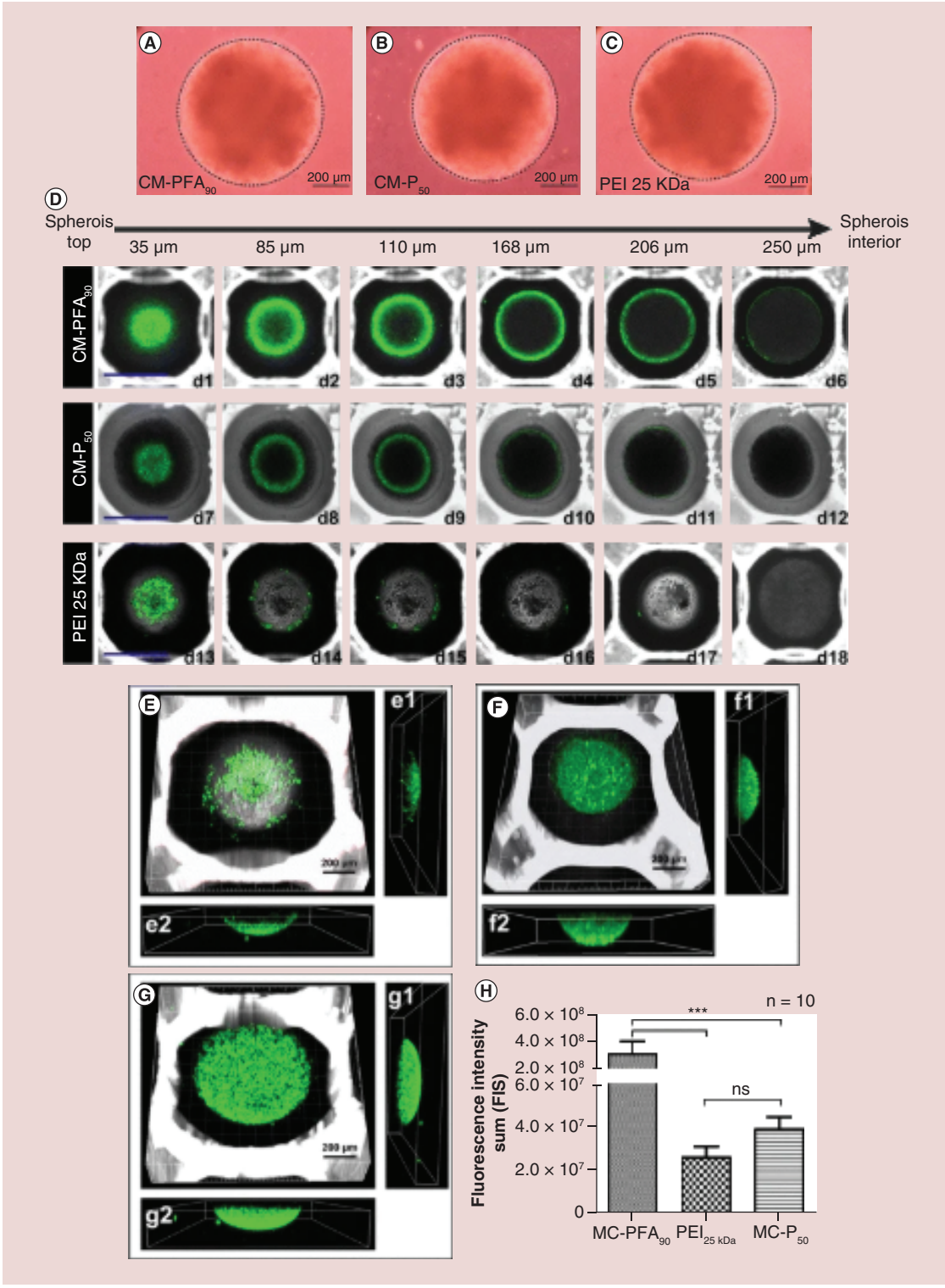

Figure 5. Influence of the corona composition of functionalized chitosan-based nanoparticles in their penetration into 3D HeLa cells spheroids. (A) Optical microscopy images of spheroids incubated with folate and PEG dual-functionalized chitosan-based nanoparticles, **(B)** nontargeted PEGylated nanoparticles and **(C)** PEI 25kDa. **(D1-D6; G, G1, G2)** Confocal images of the GFP expression in 3D spheroids mediated by the folate and PEG dual-functionalized chitosan-based nanoparticles, **(D7-D12; F, F1, F2)** nontargeted PEGylated nanoparticles and **(D13-D18; E, E1, E2)** PEI 25kDa. **(H)** GFP fluorescence intensity in 3D spheroids incubated with the different nanoparticles. Green channel: GFP expression; grey-white channel: differential interference contrast (DIC) images. Scale bar represents 700 µm.
Data is presented as mean ± SD, n = 10, ***$p < 0.001$.
$CM\text{-}PFA_{90}$/$MC\text{-}PFA_{90}$: Folate and PEG dual-functionalized chitosan-based nanoparticle; $CM\text{-}P_{50}$/$MC\text{-}P_{50}$: Nontargeted PEGylated nanoparticle; PEI: Poly(ethyleneimine).
Reproduced with permission from [88], © Springer Nature (2014).

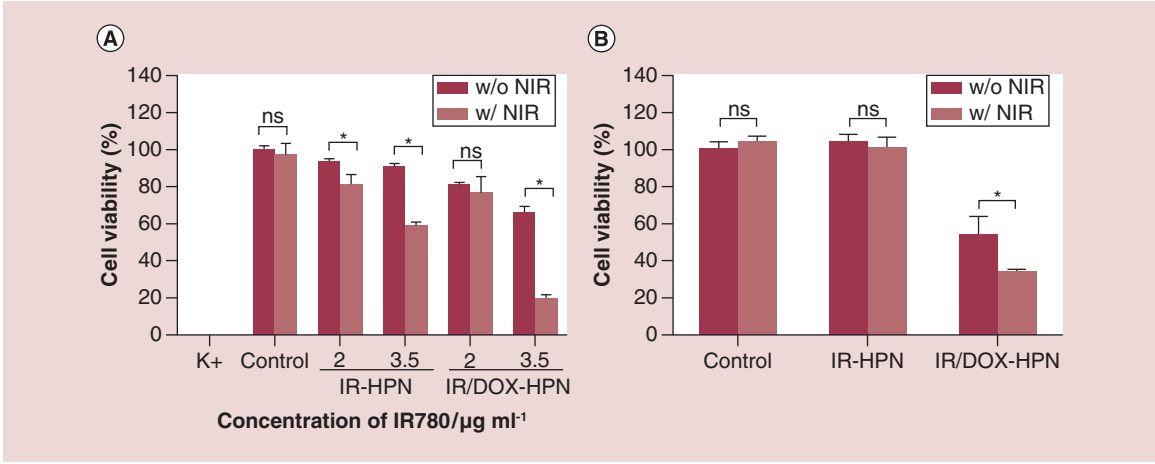

Figure 6. Comparison of the effect of chemo-photothermal therapy in 2D monolayers and 3D spheroids.
Determination of the chemo-photothermal effect mediated by IR/DOX-HPN toward **(A)** monolayers of MCF-7 cells and **(B)** MCF-7 spheroids. w/ NIR: Laser irradiation (808 nm, 1.7 W/cm^2, 5 min). w/o NIR: Non-irradiated. Data represents mean±SD, *$p < 0.0001$; ns=non-significant.
IR/DOX-HPN: DOX and IR780-loaded hyaluronic acid-based nanoparticle; IR-HPN: IR780 loaded hyaluronic acid-based nanoparticle; NIR: near infrared.
Reproduced with permission from [10], © Elsevier B.V. (2019).

next years, addressing these bottlenecks will surely increase the use of spheroids in the screening of nanomedicines. When compared with solid tumors, spheroids also lack vasculature and may not promptly present abundant cell–ECM interactions [27,37]. In this context, recently the microfluidic culture of spheroids (spheroids-on-a-chip) has been receiving an increased interest due to its capacity to mimic the vascular function [117–119]. On the other hand, hybrid 3D cultures comprised by spheroids incorporated in scaffolds/hydrogels have been engineered to readily establish cell–ECM cues and/or penetration/resistance barriers [120,121].

Overall, spheroids are a valuable 3D *in vitro* cancer model that can be used as a tool to bridge the gap between 2D *in vitro* and *in vivo* cancer models.

Executive summary

2D *in vitro* cell cultures
- 2D *in vitro* cancer models are usually used to screen the efficacy of anticancer agents.
- 2D *in vitro* models are unable to mimic the key features of solid tumors.
- 2D *in vitro* models cannot accurately predict the *in vivo* efficacy of nanomedicines.

3D *in vitro* spheroids as cancer models
- Large spheroids can mimic the solid tumors' 3D architecture, cellular heterogeneity and cell–cell and cell–extracellular matrix interactions.
- Spheroids can mimic the main therapeutics' resistance patterns of solid tumors.
- Spheroids are valuable 3D *in vitro* cancer models that can be used as a tool to bridge the gap between 2D *in vitro* and *in vivo* cancer models.

3D spheroids for the screening of nanomedicines' physicochemical properties
- Spheroids are a valuable model for optimizing the nanomedicines' physicochemical properties.
- Nanomedicines' size, charge, shape and corona composition can affect their penetration into spheroids.
- The smaller nanomedicines tend to have a higher accumulation in the spheroids' core, while the larger nanomaterials accumulate mostly in the spheroids' outer layer.

3D spheroids for evaluating the therapeutic efficacy of nanomedicines
- Spheroids have been used to evaluate nanomedicine-mediated chemo-, radio-, photothermal and photodynamic therapies and gene delivery.
- The efficacy of nanomedicines toward spheroids is generally inferior to that attained using 2D *in vitro* models.

Author contributions

I Mó, IJ Sabino and D de Melo-Diogo performed the literature revision, analyzed the data and wrote the article. R Lima-Sousa and CG Alves analyzed the data and wrote the article. IJ Correia conceived and wrote the article.

Financial & competing interests disclosure

This work was supported by FEDER funds through the POCI – COMPETE 2020 – Operational Programme Competitiveness and Internationalisation in Axis I – Strengthening research, technological development and innovation (Project POCI-01-0145-FEDER-007491) and National Funds by FCT – Foundation for Science and Technology (Project UID/Multi/00709/2013). The funding from CENTRO-01-0145-FEDER-028989 and POCI-01-0145-FEDER-031462 is also acknowledged. D de Melo-Diogo acknowledges CENTRO-01-0145-FEDER-028989 for the funding given on the form of a research contract. CG Alves and R Lima-Sousa acknowledge individual PhD fellowships from FCT (SFRH/BD/145386/2019 and SFRH/BD/144922/2019). The authors have no other relevant affiliations or financial involvement with any organization or entity with a financial interest in or financial conflict with the subject matter or materials discussed in the manuscript apart from those disclosed.

No writing assistance was utilized in the production of this manuscript.

References

Papers of special note have been highlighted as: • of interest; •• of considerable interest

1. Chidambaram M, Manavalan R, Kathiresan K. Nanotherapeutics to overcome conventional cancer chemotherapy limitations. *J. Pharm. Pharm. Sci.* 14(1), 67–77 (2011).
2. Kaminski BM, Steinhilber D, Stein JM, Ulrich S. Phytochemicals resveratrol and sulforaphane as potential agents for enhancing the anti-tumor activities of conventional cancer therapies. *Curr. Pharm. Biotechnol.* 13(1), 137–146 (2012).
3. Pais-Silva C, De Melo-Diogo D, Correia IJ. IR780-loaded TPGS-TOS micelles for breast cancer photodynamic therapy. *Eur. J. Pharm. Biopharm.* 113, 108–117 (2017).
4. Gaio E, Guerrini A, Ballestri M *et al.* Keratin nanoparticles co-delivering docetaxel and chlorin e6 promote synergic interaction between chemo-and photo-dynamic therapies. *J. Photochem. Photobiol. B* 199, 111598 (2019).
5. Ernsting MJ, Murakami M, Roy A, Li S-D. Factors controlling the pharmacokinetics, biodistribution and intratumoral penetration of nanoparticles. *J. Control. Rel.* 172(3), 782–794 (2013).
6. Blanco E, Shen H, Ferrari M. Principles of nanoparticle design for overcoming biological barriers to drug delivery. *Nat. Biotechnol.* 33(9), 941–951 (2015).
7. De Melo-Diogo D, Pais-Silva C, Dias DR, Moreira AF, Correia IJ. Strategies to improve cancer photothermal therapy mediated by nanomaterials. *Adv. Healthcare Mater.* 6(10), 1700073 (2017).
8. Alves CG, Lima-Sousa R, De Melo-Diogo D, Louro RO, Correia IJ. IR780 based nanomaterials for cancer imaging and photothermal, photodynamic and combinatorial therapies. *Int. J. Pharm.* 542(1–2), 164–175 (2018).
9. Subramani K, Hosseinkhani H, Khraisat A, Hosseinkhani M, Pathak Y. Targeting nanoparticles as drug delivery systems for cancer treatment. *Curr. Nanosci.* 5(2), 135–140 (2009).
10. Alves CG, De Melo-Diogo D, Lima-Sousa R, Costa EC, Correia IJ. Hyaluronic acid functionalized nanoparticles loaded with IR780 and DOX for cancer chemo-photothermal therapy. *Eur. J. Pharm. Biopharm.* 137, 86–94 (2019).

• **Studies the therapeutic effect of nanoparticles in 2D and 3D breast cancer models.**

11. Vaidya B, Parvathaneni V, Kulkarni NS *et al.* Cyclodextrin modified erlotinib loaded PLGA nanoparticles for improved therapeutic efficacy against non-small cell lung cancer. *Int. J. Biol. Macromol.* 122, 338–347 (2019).
12. Muddineti OS, Kumari P, Ray E, Ghosh B, Biswas S. Curcumin-loaded chitosan-cholesterol micelles: evaluation in monolayers and 3D cancer spheroid model. *Nanomedicine* 12(12), 1435–1453 (2017).
13. Quader S, Kataoka K. Nanomaterial-enabled cancer therapy. *Mol. Ther.* 25(7), 1501–1513 (2017).
14. Melo-Diogo DD, Pais-Silva C, Costa EC, Louro RO, Correia IJ. D-α-tocopheryl polyethylene glycol 1000 succinate functionalized nanographene oxide for cancer therapy. *Nanomedicine* 12(5), 443–456 (2017).
15. Zhang L, Li G, Gao M *et al.* RGD-peptide conjugated inulin-ibuprofen nanoparticles for targeted delivery of Epirubicin. *Colloids Surf. B* 144, 81–89 (2016).
16. Moreira AF, Gaspar VM, Costa EC *et al.* Preparation of end-capped pH-sensitive mesoporous silica nanocarriers for on-demand drug delivery. *Eur. J. Pharm. Biopharm.* 88(3), 1012–1025 (2014).
17. Lima-Sousa R, De Melo-Diogo D, Alves CG *et al.* Hyaluronic acid functionalized green reduced graphene oxide for targeted cancer photothermal therapy. *Carbohydr. Polym.* 200, 93–99 (2018).
18. Rodrigues CF, Reis CA, Moreira AF, Ferreira P, Correia IJ. Optimization of gold core-mesoporous silica shell functionalization with TPGS and PEI for cancer therapy. *Microporous Mesoporous Mater.* 285, 1–12 (2019).

19. De Melo-Diogo D, Costa EC, Alves CG *et al.* POxylated graphene oxide nanomaterials for combination chemo-phototherapy of breast cancer cells. *Eur. J. Pharm. Biopharm.* 131, 162–169 (2018).
20. Cai X, Luo Y, Zhang W, Du D, Lin Y. pH-sensitive ZnO quantum dots–doxorubicin nanoparticles for lung cancer targeted drug delivery. *ACS Appl. Mater. Interfaces* 8(34), 22442–22450 (2016).
21. Saadati R, Dadashzadeh S. Marked effects of combined TPGS and PVA emulsifiers in the fabrication of etoposide-loaded PLGA-PEG nanoparticles: *in vitro* and *in vivo* evaluation. *Int. J. Pharm.* 464(1–2), 135–144 (2014).
22. Farboud ES, Nasrollahi SA, Tabbakhi Z. Novel formulation and evaluation of a Q10-loaded solid lipid nanoparticle cream: *in vitro* and *in vivo* studies. *Int. J. Nanomed.* 6, 611–617 (2011).
23. Jose S, Sowmya S, Cinu T, Aleykutty N, Thomas S, Souto E. Surface modified PLGA nanoparticles for brain targeting of Bacoside-A. *Eur. J. Pharm. Sci.* 63, 29–35 (2014).
24. Imamura Y, Mukohara T, Shimono Y *et al.* Comparison of 2D-and 3D-culture models as drug-testing platforms in breast cancer. *Oncol. Rep.* 33(4), 1837–1843 (2015).
25. Costa EC, De Melo-Diogo D, Moreira AF, Carvalho MP, Correia IJ. Spheroids formation on non-adhesive surfaces by liquid overlay technique: considerations and practical approaches. *Biotechnol. J.* 13(1), 1700417 (2018).

•• **Highlights the production of spheroids by the liquid overlay technique.**

26. Longati P, Jia X, Eimer J *et al.* 3D pancreatic carcinoma spheroids induce a matrix-rich, chemoresistant phenotype offering a better model for drug testing. *BMC Cancer* 13(1), 95 (2013).
27. Costa EC, Moreira AF, De Melo-Diogo D, Gaspar VM, Carvalho MP, Correia IJ. 3D tumor spheroids: an overview on the tools and techniques used for their analysis. *Biotechnol. Adv.* 34(8), 1427–1441 (2016).

•• **Summarizes the techniques available for spheroids' characterization.**

28. Chen P, Liang H-W, Lv X-H, Zhu H-Z, Yao H-B, Yu S-H. Carbonaceous nanofiber membrane functionalized by beta-cyclodextrins for molecular filtration. *ACS Nano* 5(7), 5928–5935 (2011).
29. Li X, Li R, Qian X *et al.* Superior antitumor efficiency of cisplatin-loaded nanoparticles by intratumoral delivery with decreased tumor metabolism rate. *Eur. J. Pharm. Biopharm.* 70(3), 726–734 (2008).
30. Lv D, Hu Z, Lu L, Lu H, Xu X. Three-dimensional cell culture: a powerful tool in tumor research and drug discovery. *Oncol. Lett.* 14(6), 6999–7010 (2017).
31. Alemany-Ribes M, Semino CE. Bioengineering 3D environments for cancer models. *Adv. Drug Delivery Rev.* 79, 40–49 (2014).
32. Kimlin LC, Casagrande G, Virador VM. *In vitro* three-dimensional (3D) models in cancer research: an update. *Mol. Carcinog.* 52(3), 167–182 (2013).
33. Millard M, Yakavets I, Zorin V, Kulmukhamedova A, Marchal S, Bezdetnaya L. Drug delivery to solid tumors: the predictive value of the multicellular tumor spheroid model for nanomedicine screening. *Int. J. Nanomed.* 12, 7993–8007 (2017).
34. Sims LB, Huss MK, Frieboes HB, Steinbach-Rankins JM. Distribution of PLGA-modified nanoparticles in 3D cell culture models of hypo-vascularized tumor tissue. *J. Nanobiotechnol.* 15(1), 67 (2017).
35. Chaicharoenaudomrung N, Kunhorm P, Noisa P. Three-dimensional cell culture systems as an *in vitro* platform for cancer and stem cell modeling. *World J. Stem Cells* 11(12), 1065–1083 (2019).
36. Nunes AS, Barros AS, Costa EC, Moreira AF, Correia IJ. 3D tumor spheroids as *in vitro* models to mimic *in vivo* human solid tumors resistance to therapeutic drugs. *Biotechnol. Bioeng.* 116(1), 206–226 (2019).
37. Langhans SA. Three-dimensional *in vitro* cell culture models in drug discovery and drug repositioning. *Front. Pharmacol.* 9(6), (2018).
38. Lu H, Stenzel MH. Multicellular tumor spheroids (MCTS) as a 3D *in vitro* evaluation tool of nanoparticles. *Small* 14(13), 1702858 (2018).
39. Hashem M, Weiler-Sagie M, Kuppusamy P, Neufeld G, Neeman M, Blank A. Electron spin resonance microscopic imaging of oxygen concentration in cancer spheroids. *J. Magn. Reson.* 256, 77–85 (2015).
40. Sant S, Johnston PA. The production of 3D tumor spheroids for cancer drug discovery. *Drug Discov. Today Technol.* 23, 27–36 (2017).

•• **Describes methods for producing spheroids.**

41. Zanoni M, Piccinini F, Arienti C *et al.* 3D tumor spheroid models for *in vitro* therapeutic screening: a systematic approach to enhance the biological relevance of data obtained. *Sci. Rep.* 6(1), 1–11 (2016).
42. Huang K, Ma H, Liu J *et al.* Size-dependent localization and penetration of ultrasmall gold nanoparticles in cancer cells, multicellular spheroids, and tumors *in vivo*. *ACS Nano* 6(5), 4483–4493 (2012).

• **Demonstrates the influence of the nanoparticles' size in their penetration into 3D spheroids.**

43. Huang K, Boerhan R, Liu C, Jiang G. Nanoparticles penetrate into the multicellular spheroid-on-chip: effect of surface charge, protein corona, and exterior flow. *Mol. Pharmaceutics* 14(12), 4618–4627 (2017).
44. Sims LB, Curtis LT, Frieboes HB, Steinbach-Rankins JM. Enhanced uptake and transport of PLGA-modified nanoparticles in cervical cancer. *J. Nanobiotechnol.* 14(1), 33 (2016).

- **Demonstrates the influence of PLGA nanoparticles' coating on their penetration into spheroids.**

45. Dilnawaz F, Sahoo SK. Enhanced accumulation of curcumin and temozolomide loaded magnetic nanoparticles executes profound cytotoxic effect in glioblastoma spheroid model. *Eur. J. Pharm. Biopharm.* 85(3), 452–462 (2013).
46. Sarisozen C, Dhokai S, Tsikudo EG, Luther E, Rachman IM, Torchilin VP. Nanomedicine based curcumin and doxorubicin combination treatment of glioblastoma with scFv-targeted micelles: *In vitro* evaluation on 2D and 3D tumor models. *Eur. J. Pharm. Biopharm.* 108, 54–67 (2016).
47. Liu J, Liu K, Feng L, Liu Z, Xu L. Comparison of nanomedicine-based chemotherapy, photodynamic therapy and photothermal therapy using reduced graphene oxide for the model system. *Biomater. Sci.* 5(2), 331–340 (2017).
48. Lazzari G, Couvreur P, Mura S. Multicellular tumor spheroids: a relevant 3D model for the *in vitro* preclinical investigation of polymer nanomedicines. *Polym. Chem.* 8(34), 4947–4969 (2017).
49. Huang B-W, Gao J-Q. Application of 3D cultured multicellular spheroid tumor models in tumor-targeted drug delivery system research. *J. Control. Rel.* 270, 246–259 (2018).
50. Hamilton G, Rath B. Applicability of tumor spheroids for *in vitro* chemosensitivity assays. *Expert Opin. Drug Metab. Toxicol.* 15(1), 15–23 (2019).
51. McMahon KM, Volpato M, Chi H *et al.* Characterization of changes in the proteome in different regions of 3D multicell tumor spheroids. *J. Proteome Res.* 11(5), 2863–2875 (2012).
52. Däster S, Amatruda N, Calabrese D *et al.* Induction of hypoxia and necrosis in multicellular tumor spheroids is associated with resistance to chemotherapy treatment. *Oncotarget* 8(1), 1725–1736 (2017).
53. Laurent J, Frongia C, Cazales M, Mondesert O, Ducommun B, Lobjois V. Multicellular tumor spheroid models to explore cell cycle checkpoints in 3D. *BMC Cancer* 13(1), 73 (2013).
54. Wigerup C, Påhlman S, Bexell D. Therapeutic targeting of hypoxia and hypoxia-inducible factors in cancer. *Pharmacol. Ther.* 164, 152–169 (2016).
55. Wartenberg M, Ling FC, Müschen M *et al.* Regulation of the multidrug resistance transporter P-glycoprotein in multicellular tumor spheroids by hypoxia-inducible factor (HIF-1) and reactive oxygen species. *FASEB J.* 17(3), 503–505 (2003).
56. Wartenberg M, Hoffmann E, Schwindt H *et al.* Reactive oxygen species-linked regulation of the multidrug resistance transporter P-glycoprotein in Nox-1 overexpressing prostate tumor spheroids. *FEBS Lett.* 579(20), 4541–4549 (2005).
57. Mellor HR, Callaghan R. Accumulation and distribution of doxorubicin in tumour spheroids: the influence of acidity and expression of P-glycoprotein. *Cancer Chemother. Pharmacol.* 68(5), 1179–1190 (2011).
58. Han S-S, Li Z-Y, Zhu J-Y *et al.* Dual-pH sensitive charge-reversal polypeptide micelles for tumor-triggered targeting uptake and nuclear drug delivery. *Small* 11(21), 2543–2554 (2015).
59. Bhagat M, Halligan S, Sofou S. Nanocarriers to solid tumors: considerations on tumor penetration and exposure of tumor cells to therapeutic agents. *Curr. Pharm. Biotechnol.* 13(7), 1306–1316 (2012).
60. Goodman TT, Olive PL, Pun SH. Increased nanoparticle penetration in collagenase-treated multicellular spheroids. *Int. J. Nanomed.* 2(2), 265–274 (2007).
61. Costa EC, Gaspar VM, Marques JG, Coutinho P, Correia IJ. Evaluation of nanoparticle uptake in co-culture cancer models. *PLoS ONE* 8(7), e70072 (2013).
62. Trédan O, Galmarini CM, Patel K, Tannock IF. Drug resistance and the solid tumor microenvironment. *J. Natl. Cancer Inst.* 99(19), 1441–1454 (2007).
63. Box C, Rogers SJ, Mendiola M, Eccles SA. Tumour-microenvironmental interactions: paths to progression and targets for treatment. *Semin. Cancer Biol.* 20(3), 128–138 (2010).
64. Lamberti MJ, Rettel M, Krijgsveld J, Rivarola VA, Rumie Vittar NB. Secretome profiling of heterotypic spheroids suggests a role of fibroblasts in HIF-1 pathway modulation and colorectal cancer photodynamic resistance. *Cell. Oncol.* 42(2), 173–196 (2019).
65. Vorwald CE, Joshee S, Leach JK. Spatial localization of endothelial cells in heterotypic spheroids influences Notch signaling. *J. Mol. Med.* doi:10.1007/s00109-020-01883-1 (2020) (Epub ahead of print).
66. Yang YN, Li S, Sun Y, Zhang D, Zhao Z, Liu L. Reversing platinum resistance in ovarian cancer multicellular spheroids by targeting Bcl-2. *Onco Targets Ther.* 12, 897 (2019).
67. Sahay G, Alakhova DY, Kabanov AV. Endocytosis of nanomedicines. *J. Control. Rel.* 145(3), 182–195 (2010).
68. Zhao J, Stenzel MH. Entry of nanoparticles into cells: The importance of nanoparticle properties. *Polym. Chem.* 9(3), 259–272 (2018).
69. Tang J, Kuai R, Yuan W, Drake L, Moon JJ, Schwendeman A. Effect of size and pegylation of liposomes and peptide-based synthetic lipoproteins on tumor targeting. *Nanomedicine* 13(6), 1869–1878 (2017).
70. Zhang J, Wang X, Wen J *et al.* Size effect of mesoporous organosilica nanoparticles on tumor penetration and accumulation. *Biomater. Sci.* 7(11), 4790–4799 (2019).

71. Zhao J, Lu H, Xiao P, Stenzel MH. Cellular uptake and movement in 2D and 3D multicellular breast cancer models of fructose-based cylindrical micelles that is dependent on the rod length. *ACS Appl. Mater. Interfaces* 8(26), 16622–16630 (2016).
72. Tchoryk A, Taresco V, Argent RH *et al.* Penetration and uptake of nanoparticles in 3D tumor spheroids. *Bioconjugate Chem.* 30(5), 1371–1384 (2019).
73. Lu H, Su J, Mamdooh R, Li Y, Stenzel MH. Cellular uptake of gold nanoparticles and their movement in 3D multicellular tumor spheroids: effect of molecular weight and grafting density of poly(2-hydroxyl ethyl acrylate). *Macromol. Biosci.* 20, 1900221 (2019).
74. Lu H, Noorani L, Jiang Y, Du AW, Stenzel MH. Penetration and drug delivery of albumin nanoparticles into pancreatic multicellular tumor spheroids. *J. Mater. Chem. B* 5(48), 9591–9599 (2017).
75. Yu W, He X, Yang Z *et al.* Sequentially responsive biomimetic nanoparticles with optimal size in combination with checkpoint blockade for cascade synergetic treatment of breast cancer and lung metastasis. *Biomaterials* 217, 119309 (2019).
76. Wang H-X, Zuo Z-Q, Du J-Z *et al.* Surface charge critically affects tumor penetration and therapeutic efficacy of cancer nanomedicines. *Nano Today* 11(2), 133–144 (2016).
77. Kostarelos K, Emfietzoglou D, Papakostas A, Yang W-H, Ballangrud Å, Sgouros G. Binding and interstitial penetration of liposomes within avascular tumor spheroids. *Int. J. Cancer* 112(4), 713–721 (2004).
78. Jin S, Ma X, Ma H *et al.* Surface chemistry-mediated penetration and gold nanorod thermotherapy in multicellular tumor spheroids. *Nanoscale* 5(1), 143–146 (2013).
79. Waite CL, Roth CM. Nanoscale drug delivery systems for enhanced drug penetration into solid tumors: current progress and opportunities. *Crit. Rev. Bioeng.* 40(1), 21–41 (2012).
80. Cai R-Q, Liu D-Z, Cui H *et al.* Charge reversible calcium phosphate lipid hybrid nanoparticle for siRNA delivery. *Oncotarget* 8(26), 42772–42788 (2017).
81. Sujai PT, Joseph MM, Saranya G, Nair JB, Murali VP, Maiti K. Surface charge modulates the internalization vs penetration of gold nanoparticles: a comprehensive scrutiny on monolayer cancer cells, multicellular spheroids and solid tumor by SERS modality. *Nanoscale* 12, 6971 (2020).
82. Zhao J, Lu H, Wong S, Lu M, Xiao P, Stenzel MH. Influence of nanoparticle shapes on cellular uptake of paclitaxel loaded nanoparticles in 2D and 3D cancer models. *Polym. Chem.* 8(21), 3317–3326 (2017).
83. Dias DR, Moreira AF, Correia IJ. The effect of the shape of gold core-mesoporous silica shell nanoparticles on the cellular behavior and tumor spheroid penetration. *J. Mater. Chem. B* 4(47), 7630–7640 (2016).
84. Agarwal R, Jurney P, Raythatha M *et al.* Effect of shape, size, and aspect ratio on nanoparticle penetration and distribution inside solid tissues using 3D spheroid models. *Adv. Healthcare Mater.* 4(15), 2269–2280 (2015).
85. Zhang L, Wang Y, Yang D *et al.* Shape effect of nanoparticles on tumor penetration in monolayers versus spheroids. *Mol. Pharmaceutics* 16(7), 2902–2911 (2019).
86. Xie X, Liao J, Shao X, Li Q, Lin Y. The effect of shape on cellular uptake of gold nanoparticles in the forms of stars, rods, and triangles. *Sci. Rep.* 7(1), 1–9 (2017).
87. Wang X, Tang H, Wang C, Zhang J, Wu W, Jiang X. Phenylboronic acid-mediated tumor targeting of chitosan nanoparticles. *Theranostics* 6(9), 1378–1392 (2016).
88. Gaspar VM, Costa EC, Queiroz JA, Pichon C, Sousa F, Correia IJ. Folate-targeted multifunctional amino acid-chitosan nanoparticles for improved cancer therapy. *Pharm. Res.* 32(2), 562–577 (2015).
89. Perche F, Patel NR, Torchilin VP. Accumulation and toxicity of antibody-targeted doxorubicin-loaded PEG-PE micelles in ovarian cancer cell spheroid model. *J. Control. Rel.* 164(1), 95–102 (2012).
90. Shabana AM, Mondal UK, Alam MR *et al.* pH-sensitive multiligand gold nanoplatform targeting carbonic anhydrase IX enhances the delivery of doxorubicin to hypoxic tumor spheroids and overcomes the hypoxia-induced chemoresistance. *ACS Appl. Mater. Interfaces* 10(21), 17792–17808 (2018).
91. Liu R, Hu C, Yang Y, Zhang J, Gao H. Theranostic nanoparticles with tumor-specific enzyme-triggered size reduction and drug release to perform photothermal therapy for breast cancer treatment. *Acta Pharm. Sin. B* 9(2), 410–420 (2019).
92. Yu Q, Qiu Y, Li J *et al.* Targeting cancer-associated fibroblasts by dual-responsive lipid-albumin nanoparticles to enhance drug perfusion for pancreatic tumor therapy. *J. Control. Rel.* 321, 564–575 (2020).
93. Zhu X, Gong Y, Liu Y *et al.* Ru@ CeO_2 yolk shell nanozymes: oxygen supply in situ enhanced dual chemotherapy combined with photothermal therapy for orthotopic/subcutaneous colorectal cancer. *Biomaterials* 242, 119923 (2020).
94. Yan G, Zha Q, Wang J *et al.* Dynamic, ultra-pH-sensitive graft copolymer micelles mediated rapid, complete destruction of 3-D tumor spheroids *in vitro*. *Polymer* 111, 192–203 (2017).
95. Cheng X, Wang X, Cao Z, Yao W, Wang J, Tang R. Folic acid-modified soy protein nanoparticles for enhanced targeting and inhibitory. *Mater. Sci. Eng.* 71, 298–307 (2017).
96. Ran R, Wang H, Liu Y *et al.* Microfluidic self-assembly of a combinatorial library of single-and dual-ligand liposomes for *in vitro* and *in vivo* tumor targeting. *Eur. J. Pharm. Biopharm.* 130, 1–10 (2018).

97. He X, Chen X, Liu L *et al.* Sequentially triggered nanoparticles with tumor penetration and intelligent drug release for pancreatic cancer therapy. *Adv. Sci.* 5(5), 1701070 (2018).

98. Sarisozen C, Abouzeid AH, Torchilin VP. The effect of co-delivery of paclitaxel and curcumin by transferrin-targeted PEG-PE-based mixed micelles on resistant ovarian cancer in 3-D spheroids and in vivo tumors. *Eur. J. Pharm. Biopharm.* 88(2), 539–550 (2014).

99. Malarvizhi GL, Retnakumari AP, Nair S, Koyakutty M. Transferrin targeted core–shell nanomedicine for combinatorial delivery of doxorubicin and sorafenib against hepatocellular carcinoma. *Nanomedicine* 10(8), 1649–1659 (2014).

100. Du AW, Lu H, Stenzel MH. Core-cross-linking accelerates antitumor activities of paclitaxel-conjugate micelles to prostate multicellular tumor spheroids: a comparison of 2D and 3D models. *Biomacromolecules* 16(5), 1470–1479 (2015).

101. Lu H, Utama RH, Kitiyotsawat U, Babiuch K, Jiang Y, Stenzel MH. Enhanced transcellular penetration and drug delivery by crosslinked polymeric micelles into pancreatic multicellular tumor spheroids. *Biomater. Sci.* 3(7), 1085–1095 (2015).

102. Cheng X, Li D, Sun M *et al.* Co-delivery of DOX and PDTC by pH-sensitive nanoparticles to overcome multidrug resistance in breast cancer. *Colloids Surf. B* 181, 185–197 (2019).

103. Sadri A, Changizi V, Eivazadeh N. Evaluation of glioblastoma (U87) treatment with ZnO nanoparticle and x-ray in spheroid culture model using MTT assay. *Radiat. Phys. Chem.* 115, 17–21 (2015).

104. Xu W-H, Han M, Dong Q *et al.* Doxorubicin-mediated radiosensitivity in multicellular spheroids from a lung cancer cell line is enhanced by composite micelle encapsulation. *Int. J. Nanomed.* 7, 2661–2671 (2012).

105. Cho W, Kim MS, Lee K-H *et al.* Ionizing radiation attracts tumor targeting and apoptosis by radiotropic lysyl oxidase traceable nanoparticles. *Nanomedicine* 24, 102141 (2020).

106. Park S, Kim H, Lim SC *et al.* Gold nanocluster-loaded hybrid albumin nanoparticles with fluorescence-based optical visualization and photothermal conversion for tumor detection/ablation. *J. Control. Rel.* 304, 7–18 (2019).

107. Moreira AF, Dias DR, Costa EC, Correia IJ. Thermo- and pH-responsive nano-in-micro particles for combinatorial drug delivery to cancer cells. *Eur. J. Pharm. Sci.* 104, 42–51 (2017).

108. Nagesetti A, Srinivasan S, Mcgoron AJ. Polyethylene glycol modified ORMOSIL theranostic nanoparticles for triggered doxorubicin release and deep drug delivery into ovarian cancer spheroids. *J. Photochem. Photobiol. B* 174, 209–216 (2017).

109. Madsen SJ, Christie C, Hong SJ *et al.* Nanoparticle-loaded macrophage-mediated photothermal therapy: potential for glioma treatment. *Lasers Med. Sci.* 30(4), 1357–1365 (2015).

110. Kumari P, Jain S, Ghosh B, Zorin V, Biswas S. Polylactide-based block copolymeric micelles loaded with chlorin e6 for photodynamic therapy: *in vitro* evaluation in monolayer and 3D spheroid models. *Mol. Pharmaceutics* 14(11), 3789–3800 (2017).

111. Wu J, Feng S, Liu W, Gao F, Chen Y. Targeting integrin-rich tumors with temoporfin-loaded vitamin-E-succinate-grafted chitosan oligosaccharide/d-α-tocopheryl polyethylene glycol 1000 succinate nanoparticles to enhance photodynamic therapy efficiency. *Int. J. Pharm.* 528(1), 287–298 (2017).

112. Jin G, He R, Liu Q *et al.* Theranostics of triple-negative breast cancer based on conjugated polymer nanoparticles. *ACS Appl. Mater. Interfaces* 10(13), 10634–10646 (2018).

113. Gaspar VM, Baril P, Costa EC *et al.* Bioreducible poly(2-ethyl-2-oxazoline)-PLA-PEI-SS triblock copolymer micelles for co-delivery of DNA minicircles and Doxorubicin. *J. Control. Rel.* 213, 175–191 (2015).

114. Gaspar VM, Gonçalves C, De Melo-Diogo D *et al.* Poly(2-ethyl-2-oxazoline)-PLA-g-PEI amphiphilic triblock micelles for co-delivery of minicircle DNA and chemotherapeutics. *J. Control. Rel.* 189, 90–104 (2014).

115. Oliveira MS, Aryasomayajula B, Pattni B, Mussi SV, Ferreira LaM, Torchilin VP. Solid lipid nanoparticles co-loaded with doxorubicin and α-tocopherol succinate are effective against drug-resistant cancer cells in monolayer and 3-D spheroid cancer cell models. *Int. J. Pharm.* 512(1), 292–300 (2016).

116. Nath S, Devi GR. Three-dimensional culture systems in cancer research: Focus on tumor spheroid model. *Pharmacol. Ther.* 163, 94–108 (2016).

117. Ko J, Ahn J, Kim S *et al.* Tumor spheroid-on-a-chip: a standardized microfluidic culture platform for investigating tumor angiogenesis. *Lab Chip* 19(17), 2822–2833 (2019).

118. Nashimoto Y, Okada R, Hanada S *et al.* Vascularized cancer on a chip: the effect of perfusion on growth and drug delivery of tumor spheroid. *Biomaterials* 229, 119547 (2020).

119. Moshksayan K, Kashaninejad N, Warkiani ME *et al.* Spheroids-on-a-chip: recent advances and design considerations in microfluidic platforms for spheroid formation and culture. *Sens. Actuators B* 263, 151–176 (2018).

120. Ho WJ, Pham EA, Kim JW *et al.* Incorporation of multicellular spheroids into 3-D polymeric scaffolds provides an improved tumor model for screening anticancer drugs. *Cancer Sci.* 101(12), 2637–2643 (2010).

121. Monteiro MV, Gaspar VM, Ferreira LP, Mano JF. Hydrogel 3D *in vitro* tumor models for screening cell aggregation mediated drug response. *Biomater. Sci.* doi:10.1039/C9BM02075F (2020) (Epub ahead of print).